Trees (2022) 36:849–861
https://doi.org/10.1007/s00468-021-02254-0

ORIGINAL ARTICLE

Influence of climate on annual changes in Douglas-fir stem taper

D. A. Jones[1] · C. A. Harrington[1] · J. B. St. Clair[2]

Received: 30 July 2021 / Accepted: 3 December 2021 / Published online: 4 January 2022

Abstract

Key message **Planting sites that are cooler, with more precipitation, early springs, high TD and hot dry summers reduce bole taper in young Douglas-fir trees. Seed-source climates that are drier, with high TD and low snowfall produce seed-sources with lower taper.**

Abstract Analysis of a 10 year reciprocal transplant study was performed to determine the influence of seed-source and local planting site climates on the bole taper of 8995 Douglas-fir (*Pseudotsuga menziesii* var. *menziesii*) trees. Trees were planted at 9 sites across Oregon and Washington, with 120 known families taken from 12 seed-source regions across California, Oregon, and Washington. Diameter at breast height (DBH) ranged from 0.1 to 22.9 cm, with tree ages ranging from 2 year-old seedlings to 12 year-old trees. Changes in Gini coefficients (ΔG) of diameters along tree boles, as a surrogate for changes in taper, were modeled as a function of age, site climate, and seed-source climate (Wang et al., in PLoS One 11, 2016) using universal response functions (URF) (Wang et al., in Ecol Appl 20:153–163, 2010). Lower Gini coefficients come from less tapered boles, i.e., more cylindrically shaped boles. There was significant influence on taper from five site climate variables: mean annual temperature (MAT), mean annual precipitation (MAP), beginning of frost-free period (bFFP), difference between minimum and maximum monthly temperatures (TD), and summer heat-moisture index (SHM). These results suggest that cooler years with more precipitation, early springs, large TD and hot dry summers reduce tree taper. There was significant influence on taper from three seed-source climate variables: percent precipitation as snow (PAS), Hargrave's climate moisture deficit (CMD), and TD. These results suggest dry regions with large ranges in monthly temperatures and low snowfall will produce seed-sources with lower Gini coefficients. Projections under future climates using an ensemble model show areas where G estimates are currently highest showed increases in G, while areas with the lowest G estimates decreased. Most of the Douglas-fir region shows declines in Gini coefficients under high emissions scenarios. These predicted changes in taper have direct implications for wood volume and carbon mass estimates of trees under future climates.

Keywords Taper · Climate change · Douglas-fir · Modeling

Introduction

Tree taper, the relative change in bole diameter as a function of stem height above the ground, is an important tree characteristic to account for when estimating wood volume, biomass, or carbon. Typically, most tree biomass is found within the bole (Poorter et al. 2012), and therefore, we can expect that changes in taper will lead to changes in total biomass of trees that are otherwise the same size (e.g., same height and diameter). This change in biomass would be predicted because a tree with higher taper will have less total volume than a tree with lower taper. This relationship between taper and tree biomass also has implications for wood, and carbon production in forests.

Changes in tree bole taper have been correlated with changes in wind loading (King 1986; Bruchert and Gardiner 2006), alteration of tree crown characteristics (Valentine et al. 2012), increased competition (del Río et al. 2019), and climate variables (Nigh and Smith 2012; Schneider et al. 2018). Douglas-fir (*Pseudotsuga menziesii* var. *menziesii*) is a globally important commercial species that has been shown to alter height growth (St Clair et al. 2005; Leites et al. 2012), diameter growth (Vejpustková and Čihák

Communicated by Vospernik.

✉ D. A. Jones
dryw.jones@usda.gov

[1] US Forest Service PNWRS, Olympia, WA, USA

[2] US Forest Service PNWRS, Corvallis, OR, USA

2019), and height–diameter relationships (St Clair et al. 2005) in response to changes in growth environments. If these changes in growth are not evenly distributed along the bole, then the cumulative impact of these site climate changes would lead to changes in tree stem taper. Many of these studies are in mature stands and do not account for early growth patterns which may play an important role in the development of tree bole taper.

Douglas-fir populations are generally considered to be closely adapted to their local climates (Rehfeldt 1994). Seedling studies have found significant relationships between Douglas-fir traits and regional climate (average climate for a group of seed-sources from similar geographic regions) in the form of local geography (Sorensen 1983; Campbell and Sugano 1993). Differences in height–diameter relationships have also been found in Douglas-fir seedlings related to seed-source climate (St Clair et al. 2005). If these differences in height–diameter relationships indicate unequal growth in diameter along the bole, then we would expect differences in bole taper between seed-sources grown in a common environment.

The presence of significant interactions between seed-source or regional climate and planting site climate is unclear with results from a Douglas-fir provenance test finding no significant interaction between seed-source and planting climates (White and Ching 1985), while a larger and longer term study found significant interaction between site and region (Krakowski and Stoehr 2009). The discrepancy in these studies may be due to differences in sample size, as the variation explained by region was small at 1–6% of the total in the Krakowski and Stoehr (2009) and small differences are hard to detect without large sample sizes. Considerable differences in ranked trait response were also noted over time in the Karkowski and Stoehr (2009) study suggesting that trees may have different rates of response climate factors at different ages. Determining the significance of interactions between seed-source and site climate is an important part of any reciprocal transplant study as those interactions can significantly impact tree trait response to changes in climate or seed-source movement. More importantly, studies determining not just if, but how, seed-source and planting site climates impact distribution of growth along the bole are lacking.

Mapping trait response to given inputs, a useful tool for visualizing and mapping genetic variation, and the range of potential response to future climates, is aided by having a single response surface (e.g., tree height growth). As tree taper defines the distribution of diameters along the bole, determining a single variable that represents taper requires finding a metric that represents that distribution of diameters. One potential metric that has been used widely in many different fields of study is the Gini coefficient (Ceriani and Verme 2012), and has been used to describe diameter and height distributions over time within tree stands (McGown et al. 2016). In the context of tree bole taper, low Gini coefficients (G) result from trees with relatively equal diameters along the bole (less taper), and higher G estimates result from trees with less equal diameters along the bole, with larger diameters closer to the base of the tree (more taper). This logical connection between Gini coefficients and taper makes Gini coefficients an excellent choice as a surrogate to taper.

Understanding how tree traits will shift in response to changes in climate is becoming an important area of research. Several climate models exist that estimate various climate metrics in historical and future contexts, but the most robust estimates come from incorporating predictions from more than one climate model into a single model called an ensemble model (Wang et al. 2016). These climate ensemble model predictions have been used to associate tree trait responses to local climates, and historical seed-source, or regional climate normals using universal response functions (URFs) (Wang et al. 2010) to predict how trees will respond to climate shifts in the future. Modeling plant trait response to future climates using ensemble models can reduce bias compared to using a single model (Yun et al. 2017). To date this approach has not been used to model tree taper response yet it could similarly reduce potential bias in projections under future climates.

Using data from a large reciprocal transplant study called the Douglas-fir Seed-Source Movement Trial (DF-SSMT) designed to look at Douglas-fir population and family responses to differences in climate, we set out to determine the following questions:

(1) What are the climate variables that best predict changes in tree taper and how do they impact taper?

(2) What is the relative explanatory power of seed-source population, region, and site in relation to predicting changes in tree bole taper?

(3) What is the range of variability in Douglas-fir tree taper for populations exposed to a common climate, local climates, and potential future climates?

Materials and methods

Study area and tree data

As part of a larger study (Bansal et al. 2015), Douglas-fir seed was collected from 120 open pollinated families from regions representing a wide range of climates (Fig. 1), grown in pots for a season, then a total of 8995 2 year-old seedlings were outplanted in cleared sites during the Fall of 2008, and early 2009 in a 3.6 square spacing, in blocks of 20 trees from each region. Sample sizes by site are shown in Table 1. Diameter, and height data were collected at the

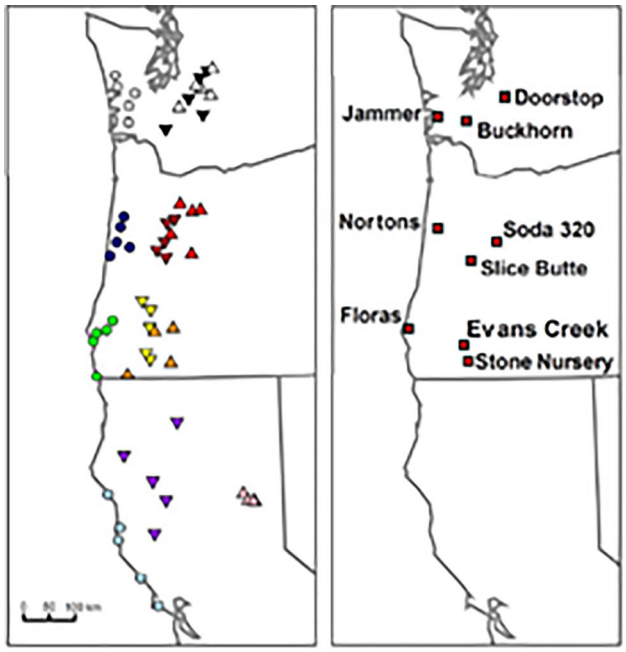

Fig. 1 Seed- source locations are shown in the map on the left, and planting site locations are shown in the map on the right. Symbols are used to differentiate between seed-source regions. The seed-source regions are: CACST (light blue circles), CAKLA (purple triangles), CASIERRA (pink triangles), ORCSTS (green circles), ORSISL (yellow triangles), ORSISH (orange triangles), ORCSTN (dark blue circles), ORCASL (dark red triangles), ORCASH (red triangles), WACST (white circles), WACASL (black triangles), WACASH (white triangles)

end of each growing season between 2009 and 2018 at nine planting sites from the DF-SSMT (Fig. 1). The seed-sources were grouped into 12 regions: California coast (CACST), California Klamath (CAKLA), California Sierra (CASIERRA), Oregon coast south (ORCSTS), Oregon Siskiyou low elevation (ORSISL), Oregon Siskiyou high elevation (ORSISH), Oregon coast north (ORCSTN), Oregon Cascades low elevation (ORCASL), Oregon Cascades high elevation (ORCASH), Washington coast (WACST), Washington Cascades low elevation (WACASL), and Washington Cascades high elevation (WACASH). Tree heights and diameter at 1.3 m bole height (DBH) were recorded for all trees in each period where a given measurement was possible, heights were measured with height poles and diameters with diameter tapes to the nearest cm for height and mm for DBH. Basal diameter was recorded to the nearest mm for all years prior to trees reaching 1.3 m, and for a subset of trees in years after trees reached 1.3 m in height, diameter at base of previous years shoot growth was also recorded for a subset of trees. Any missing tree measurements were imputed using a growth function fit to individual tree data. Average data for all trees in the study across all time periods are shown in Table 1, along with summary climate data.

Air temperature (°C) and precipitation (mm) data were collected at 30 min intervals throughout the study time period at all planting sites. In some instances, recording devices failed and this missing data was imputed using additional devices on the same site, or calibrated data from nearby weather stations from the NOAA Integrated Surface Hourly Database, and the NOAA hourly precipitation database. Missing data over the study period was less than 2% for air temperatures and less than 1% for precipitation. ClimateWNA software version 5.4 (Wang et al. 2016) was used to derive climate normals (1961–1990) for the locations the seed-sources were from (left side of Fig. 1) to represent the environmental conditions the seed-sources were adapted to. The software was also used to derive gridded climate data for future scenarios RCP4.5—low emissions and RCP8.5—high emissions scenarios (Collins et al. 2013) in years 2050 and 2080. ClimateWNA produces a large suite of annual climate variables but for this study, we focused on a smaller suite of variables, specifically: MAT (mean

Table 1 Average tree and planting site metrics

Site name	Tree height (m)	Average diameter (cm)	Tree DBH (cm)	MAT (°C)	MAP (mm)	Elevation (m)	*n*
Floras	3.73 (2.06)	4.1 (3.9)	5.8 (5.3)	11 (0.7)	2970 (737)	400	867
Stone Nursery	3.51 (1.66)	4 (3.7)	5.8 (5)	12.2 (0.7)	442 (146)	415	1087
Evans Creek	3.50 (1.75)	3.5 (3)	4.9 (4.4)	11.8 (0.8)	810 (230)	700	876
Nortons	4.63 (2.63)	5 (4.9)	7.4 (6.5)	10.6 (0.7)	1650 (403)	185	1090
Slice Butte	4.12 (2.26)	3.9 (3.7)	5.7 (4.9)	11.4 (0.7)	1410 (250)	380	873
Soda	3.12 (1.83)	2.9 (2.9)	4.1 (3.7)	10.2 (0.9)	1820 (583)	850	1108
Jammer	4.17 (2.36)	4.5 (4.5)	6.6 (5.9)	10.2 (0.6)	1940 (275)	175	876
Buckhorn	4.42 (2.46)	4.4 (4.4)	6.8 (5.7)	10.2 (0.7)	1340 (191)	240	1101
Doorstop	2.92 (1.58)	2.9 (2.9)	4 (3.6)	8.5 (0.7)	1500 (580)	860	1117

Mean values for total tree height, average of all measured diameters, tree diameter at breast height (DBH), site mean annual temperature (MAT), mean annual precipitation (MAP) followed by standard deviations in parentheses, site elevation is also shown. DBH values were measured at 1.3 m and tree diameter measures were at variable heights. Averages are for all observations

annual temperature in °C), MAP (mean annual precipitation in mm), MWMT (mean warmest month temperature °C), MCMT (mean coldest month temperature °C), TD (temperature difference between MWMT and MCMT °C), MSP (mean annual summer precipitation mm), AHM (annual heat-moisture index), and SHM (summer heat-moisture index), bFFP (beginning of frost-free period), eFFP (end of frost-free period), and PAS (percent precipitation as snow). These variables represent most of the annual climate variables in WNA, and the remaining annual variables are derived from these so including additional variables would result in autocorrelation between variables in the model. Annual estimates for the chosen climate variables were also derived from site weather data so that seed-source climate normals and annual site climate had comparable metrics.

Modeling

Deriving bole diameter Gini coefficients (G) for each tree and year required first estimating tree bole diameters (D_{tj}) as a function of relative height (RH) and basal diameter (BD_{tj}) using a taper model fit to each tree in each year (see supplementary material Sup. Equ. 1). This model was used to predict diameters along the bole for each tree in each year from a RH of 0 to 1 in RH increments of 0.001 creating a smooth taper profile data from which Gini coefficients could be calculated (see supplementary material for more information on this calculation). The resulting G values represent how unequal diameter distributions are along the bole and are mathematically bounded between completely equal distributions ($G=0$), or a perfectly cylindrical bole, and completely unequal distributions ($G=1$). Tree growth makes it impossible for G estimates to reach either of these extremes as a perfectly cylindrical tree would require all growth to stop at the lower portion of the bole, and a tree with only growth at the base could not support the weight of a crown, therefore, the model can encompass all physiologically possible values.

Predicted G estimates used for mapping of variation under different climate scenarios were derived from summing annual time step predictions from an ensemble model which took the form shown in Eq. 1. We then added these sums to a G value map interpolated from the initial G estimates for seed-sources. M in the following equation represents a matrix of URF model estimates from the best URF models fit to Sup. Equ 3:

$$\Delta G_{tj} = A\left(1 + A_{\mathrm{t}} + M\right) + B + \varepsilon. \quad (1)$$

All modeling was performed using the nlme package (Pinheiro et al. 2019) in the R statistical platform (R Core Team 2019). Several models were tested to determine the final best-fit ensemble model; see supplemental material for more detail. Maps showing seed-source response to a shared environment, and seed-source response to ten-years of growth under local site environments were created using QGIS 3.6.3 software (QGIS Development Team 2019) with the gridded data from ClimateWNA, and from raster data calculated using predictions from the best-fit ensemble model with the raster package (Hijmans 2020).

Results

Summaries of Gini coefficients of diameter distribution along the bole and tree height for study trees by region in year 1 and year 10 (Table 2) show similar values for both metrics between regions in year 1 but higher variability by year 10. Regional averages maintained their relative ranking in G and HT between year 1 to year 10. G estimates ranged from 0.291 to 0.300 in year 1 and 0.338 to 0.389 in year 10. HT ranged from 40 to 60 cm in year 1 and 419 to 740 cm in year 10, while D ranged from 1.11 to 1.43 cm in year 1 to 9.1 to 15 cm in year 10.

Mean HT and G estimates increased over time when averaged by planting site (Table 3) as they did when grouped by region. Averages grouped by site had a lower range of variation in G, but a higher range of variation in HT compared to the averages grouped by region. G estimates ranged from 0.294 to 0.302 in year 1 and from 0.360 to 0.396 in year 10. HT values ranged from 46 to 68 cm in year 1 and from 470 to 819 cm by year 10, while D ranged from 1.06 to 1.85 cm in year 1 to 9.64 to 17.4 cm in year 10.

Average BIC values for models that contained a given climate variable are shown in Table 4. The values are averaged for models in which the given climate variable was used as a site climate variable (site), or as a seed-source climate variable in the top 147 URF models, the models that were significantly better than the means model. Site ΔBIC showed higher variability than did region ΔBIC indicating that there was greater separation in the predictive power of site climate variables than seed-source climate variables between the models compared. This separation is also reflected in the BIC rank columns with site ΔBIC demonstrating clear separation in ranking while seed-source ΔBIC does not.

Average BIC ranking was not necessarily predictive of which model made it into the final ensemble model (Sup. Table 1). The site climate variables that are represented in URFs used for the final ensemble model were SHM, MAP, MAT, TD, bFFP, and the seed-source climate variables were PAS, TD, and CMD (Sup. Table 1). Within the URF models in the final ensemble model site variables SHM, MAP, MAT (above 14.7 °C) and TD were negatively correlated with changes in G, while bFFP was negatively correlated for values below 100 and positively correlated above 100, with MAT positively correlated below 14.7 °C. Within URFs in the

Table 2 Average Gini coefficients, tree heights, and diameters by region

Region	G_1	G_{10}	HT_1 (m)	D_1 (cm)	HT_{10} (m)	D_{10} (cm)
CACST	0.296 (0.000)	0.382 (0.001)	0.52 (0.01)	1.25 (0.02)	6.36 (0.07)	12.7 (0.2)
CAKLA	0.294 (0.000)	0.365 (0.001)	0.46 (0.01)	1.22 (0.01)	5.79 (0.06)	12.4 (0.2)
CASIERRA	0.291 (0.000)	0.338 (0.001)	0.40 (0.01)	1.11 (0.01)	4.19 (0.05)	9.1 (0.2)
ORCSTS	0.299 (0.000)	0.388 (0.001)	0.52 (0.01)	1.43 (0.01)	6.57 (0.06)	15.0 (0.2)
ORSISL	0.296 (0.000)	0.386 (0.001)	0.58 (0.01)	1.35 (0.02)	7.25 (0.07)	14.0 (0.2)
ORSISH	0.295 (0.000)	0.372 (0.001)	0.59 (0.01)	1.26 (0.01)	7.40 (0.08)	12.5 (0.2)
ORCSTN	0.299 (0.000)	0.388 (0.001)	0.56 (0.01)	1.41 (0.01)	7.12 (0.06)	14.9 (0.2)
ORCASL	0.298 (0.000)	0.389 (0.001)	0.48 (0.01)	1.42 (0.01)	5.80 (0.06)	15.0 (0.2)
ORCASH	0.297 (0.000)	0.377 (0.001)	0.52 (0.01)	1.30 (0.01)	6.55 (0.06)	13.4 (0.1)
WACST	0.300 (0.000)	0.389 (0.001)	0.50 (0.01)	1.40 (0.02)	6.26 (0.06)	14.4 (0.2)
WACASL	0.298 (0.000)	0.384 (0.001)	0.56 (0.01)	1.30 (0.01)	6.98 (0.06)	13.6 (0.2)
WACASH	0.295 (0.000)	0.382 (0.001)	0.60 (0.01)	1.23 (0.01)	7.33 (0.07)	12.7 (0.2)

Summary data for Gini coefficients (G), tree heights, and observed diameters by region. G_1 and G_{10} refer to average G values in year 1 and year 10, respectively. HT_1 and HT_{10} refer to average tree height values for year 1 and year 10, respectively, while D_1 and D_{10} refer to average tree diameters (basal and breast-height diameters) in year 1 and year 10, respectively. Regions represented are California coast (CACST), California Klamath (CAKLA), California Sierra (CASIERRA), Oregon Coast south (ORCSTS), Oregon Siskiyou low elevation (ORSISL), Oregon Siskiyou high elevation (ORSISH), Oregon Coast north (ORCSTN), Oregon Cascades low elevation (ORCASL), Oregon Cascades high elevation (ORCASH), Washington Coast (WACST), Washington Cascades low elevation (WACASL), and Washington Cascades high elevation (WACASH). Values in parenthesis are standard errors of the associated mean

Table 3 Summary data for average Gini coefficients and tree heights and diameters by planting location

Site name	G_1	G_{10}	HT_1 (cm)	D_1 (cm)	HT_{10} (cm)	D_{10} (cm)
Floras	0.297 (0.000)	0.379 (0.001)	52.5 (0.4)	1.4 (0.01)	643.5 (5.5)	14.1 (0.17)
Evans Creek	0.295 (0.000)	0.388 (0.001)	49.5 (0.4)	1.21 (0.01)	582.6 (3.8)	11.8 (0.10)
Stone Nursery	0.302 (0.000)	0.364 (0.001)	67.6 (0.6)	1.85 (0.02)	557.6 (4.3)	13.1 (0.11)
Nortons	0.296 (0.000)	0.396 (0.001)	52.2 (0.4)	1.36 (0.01)	819.4 (5.5)	17.4 (0.15)
Slice Butte	0.295 (0.000)	0.380 (0.001)	49.6 (0.4)	1.12 (0.01)	714.5 (5.3)	13.1 (0.12)
Soda	0.294 (0.000)	0.365 (0.001)	46.3 (0.4)	1.06 (0.01)	529.1 (5.1)	9.64 (0.11)
Jammer	0.296 (0.000)	0.393 (0.001)	51.2 (0.4)	1.33 (0.01)	739.4 (5.8)	16.3 (0.17)
Buckhorn	0.296 (0.000)	0.386 (0.001)	51.4 (0.4)	1.23 (0.01)	786.4 (4.5)	15.5 (0.12)
Doorstop	0.295 (0.000)	0.360 (0.001)	49.9 (0.4)	1.19 (0.01)	469.6 (4.3)	9.35 (0.11)

Summary data for Gini coefficients (G) and tree heights by planting locations. G_1 and G_{10} refer to average G values in 2009 and 2018 respectively. HT_1 and HT_{10} refer to average tree heights in 2009 and 2018, respectively, and D_1 and D_{10} refer to the average of diameter measurements (basal and breast-height) in year 1 and 10, respectively. Values in parenthesis are standard errors of the associated mean

ensemble model negative correlations between seed-source climate variables and changes in G were observed for CMD, and TD values below 11.5 °C, while positive correlations with changes in G were observed for PAS and TD values above 11.5 °C. Of the site climate variables represented in the final ensemble model only SHM, and MAT have rankings in the top half of URF models. Seed-source climate variables CMD and TD were both in the top half of URF models, while PAS was not. These results suggest complex interactions between the underlying climate variables and tree diameter Gini coefficients. The best-fit ensemble model form is shown as follows with parameter estimates shown in Sup. Table 2:

$$\text{Ensemble model}: \ \Delta G = A\left(1 + A_{\mathrm{t}} + M_{26} + M_{132} + M_{67} + M_{79} + M_{92}\right) + \sigma_{SRFT}.$$

Table 4 Summary of BIC values for models using the listed climate variables

Climate variable	Site ΔBIC	Site BIC rank	Seed-source ΔBIC	Seed-source BIC rank
AHM	49 (4)	137.9	880 (786)	80.2
bFFP	442 (7)	98.0	891 (773)	76.5
CMD	1450 (9)	33.0	892 (788)	75.5
eFFP	152 (9)	124.0	884 (774)	79.3
eREF	2445 (16)	7.0	888 (787)	76.8
MAP	− 10 (30)	149.1	881 (784)	79.1
MAT	818 (15)	72.0	875 (776)	80.6
MCMT	242 (9)	111.0	881 (773)	79.8
MSP	1356 (17)	46.0	884 (784)	77.6
MWMT	1110 (11)	59.0	882 (780)	78.7
PAS	–	–	872 (776)	82.4
SHM	1870 (6)	20.0	879 (783)	80.2
TD	677 (16)	85.0	900 (774)	73.8

The table shows the average values for models containing a given climate variable as a site climate variable (Site), and separate averages for models containing the same variable as a seed-source climate variable. Site or seed-source ΔBIC refers to the average difference in BIC values for models with a given climate variable used as the site or seed-source climate variable in a model compared to the means only model. Standard deviations in model BIC values are shown in parenthesis next to their respective mean estimates. BIC ranks indicate the average model rank for the given climate variable as either a site or seed-source climate variable in the URF models. BIC values are only taken from models that performed significantly better than the means only model. PAS was not measured for sites so is not included in the analysis as a site climate variable. Variables are annual heat-moisture index (AHM), day of year on which frost-free period begins (bFFP), Hargreaves climatic moisture deficit (CMD), Hargreaves reference evaporation (eREF), mean annual precipitation (MAP), mean annual temperature (MAT), mean coldest month temperature (MCMT), mean summer precipitation (MSP), mean warmest month temperature (MWMT), precipitation as snow (PAS), summer heat-moisture index (SHM), temperature difference between MWMT and MCMT (TD)

Change in Gini coefficient (ΔG) as a function of URF model estimates multiplied by a coefficient matrix (A) including an intercept term, with nested random effects (σ) at the site (S), region (R), family (F), and tree (T) level. Individual model URF parameter estimates are found in Sup. Table 1, and ensemble parameter estimates are found in Sup. Table 2.

The impact of changing individual climate variables on taper profiles is shown in Fig. 3. The curves in Fig. 3. are derived from the observed data (G_O), modeling the response of the study trees to a decade of growth under either the 95th (G_{95}), or 5th (G_5) percentile of the indicated climate variable while all other variables are taken from observations from the study. This figure demonstrates the sensitivity of tree taper to fluctuations in a single climate variable while controlling all other variables. They should not be confused with encompassing the full response of tree taper to changes in climate as that would result in changes in all of the climate variables in the model rather than just one. However, we can see from Fig. 3 that tree taper is most sensitive to SHM-site, followed by MAT-site, TD-site, MAP-site, TD-region, and finally bFFP-site as judged by the range in G values between G_{95} and G_5. Neither PAS nor CMD for region showed differences at the quantiles used in the graph so were not shown. This does not mean that those climate variables do not influence taper, given the significant influence on model BIC we know that they have an impact, but at the given percentiles, these variables did not result in noticeably different profiles possibly due to the quadratic form of the URFs used. The shift in distributions of modeled tree tapers for the different percentiles tested is not necessarily uniform indicating that at the margins of the distribution trees may respond differently to a given climate variable. For instance, the graph of the TD-region shows the 5th percentile distribution is entirely encompassed by the 95th percentile indicating that while the 95th percentile curve shows slightly more taper, the overall response also increases variation in taper across the study trees. It is important to point out that even small differences in G values can be important as these averages represent the response of all of our collected seed-sources to changes in only one climate variable, implying the potential for larger changes when more than one variable shifts across the majority of the coast Douglas-fir range as would be expected under broader changes in climate.

The shared climate map (Sup Fig. 2) shows the variation that can be attributed to the seed-sources selected for this

study when their growth environment is held at a constant shared value for a decade. G estimates ranged from 0.397 to 0.469 with larger values generally present toward the interior of the coast Douglas-fir range and smaller values generally toward the coast. Larger *G* estimates equate to less equal diameter distributions along the tree bole, or more tapered trees. The mean *G* value for the shared climate trees was 0.416, with a standard deviation of 0.008. The central location choice (green dot in Sup Fig. 2) alters the final map predictions as some populations respond more to certain climate variables (10 year weather response), however, this location is at the approximate center of the coast Douglas-fir range for the study and so was used for the final map. Using a shared site climate, this map gives some indication of the population level variation that exists in the seed-sources used in this study, though it is not a realistic response over time, as far greater variability in annual climate would be expected over a decade than occurs in this analysis.

Estimated Gini coefficients for 2020 using ClimateWNA climate variable estimates are shown in Sup. Fig. 3. *G* estimates were derived similarly to Sup. Fig. 2, with the difference being that planting site climate variables from ClimateWNA 2020 were location specific rather than estimates from a shared location. The variation in *G* shown in Sup. Fig. 3, representing the variation from seed-source and site climates, is higher than in Sup. Fig. 2 with the lowest *G* estimates equal to 0.137, and the highest equal to 0.497 with a standard deviation of 0.053. Despite the model being applied to climates outside of those in the study these values are not far from the *G* estimates for this study of 0.127–0.473, and a standard deviation of 0.036. The lowest *G* estimates (least tapered) are shown in the lower elevations in the interior of California where Douglas-fir prevalence is low. Larger *G* estimates are found at the coasts and eastern portions of the Douglas-fir range in Washington and Oregon. Trees from lower elevations in the middle of the Douglas-fir range of Oregon have lower *G* estimates than trees from the Oregon coast with trees from this state demonstrating moderate variation. Trees in Washington show the least variation of the three states shown with patches of relatively low *G* estimates in the middle of the Douglas-fir range in Washington, and relatively high *G* estimates at the coasts and higher elevations of the range, but relatively similar *G* estimates in the rest of the state.

The range of Gini coefficient values in Sup. Fig. 3 also represents large changes in potential wood volume for trees with the same height and diameter (Fig. 2). The lowest *G* estimates on the map are 134% higher in relative volume compared to the highest *G* estimates. While the 2020 map is not a representation of actual *G* estimates for locations as we did not measure all populations and used ClimateWNA estimates rather than measured values for site climate, the map does give us some indication of potential ranges of response in tree taper to a given climate regime. The range

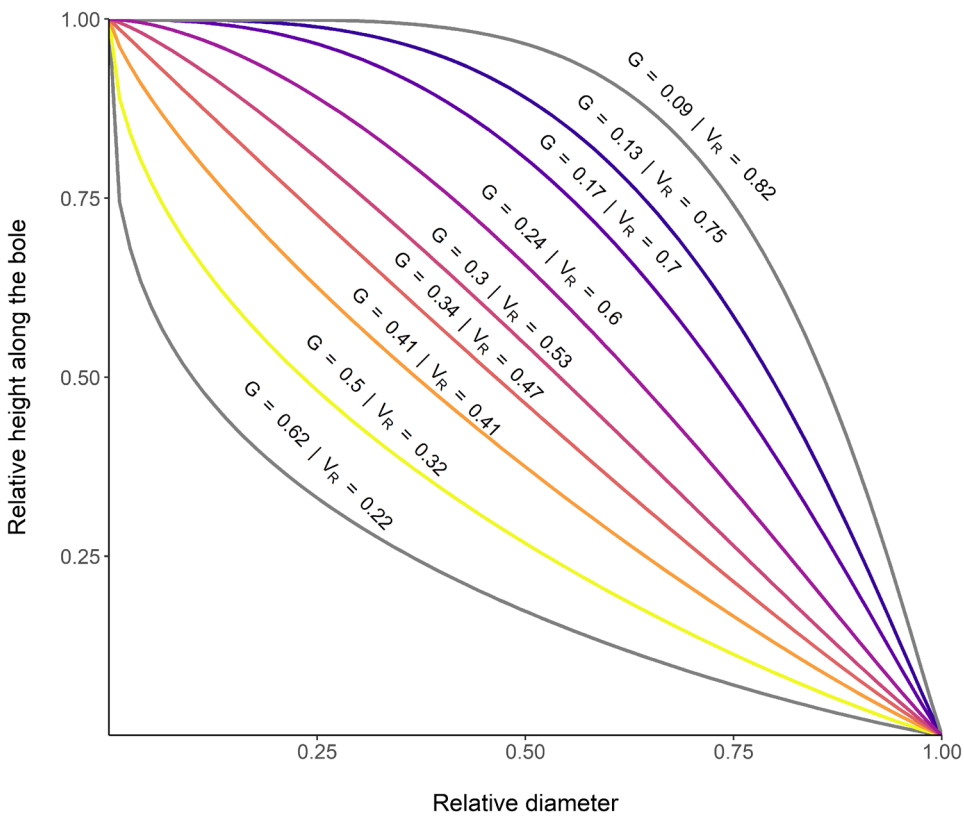

Fig. 2 Potential taper profiles for trees with associated Gini values. Relative volume indicates the sum of area under the taper profile curve. In general, the lower the Gini value is the higher the corresponding relative volume is. Given trees with identical height and diameters larger relative volume means more bole volume. Gray indicates values outside of the range shown in Sup. Fig. 3

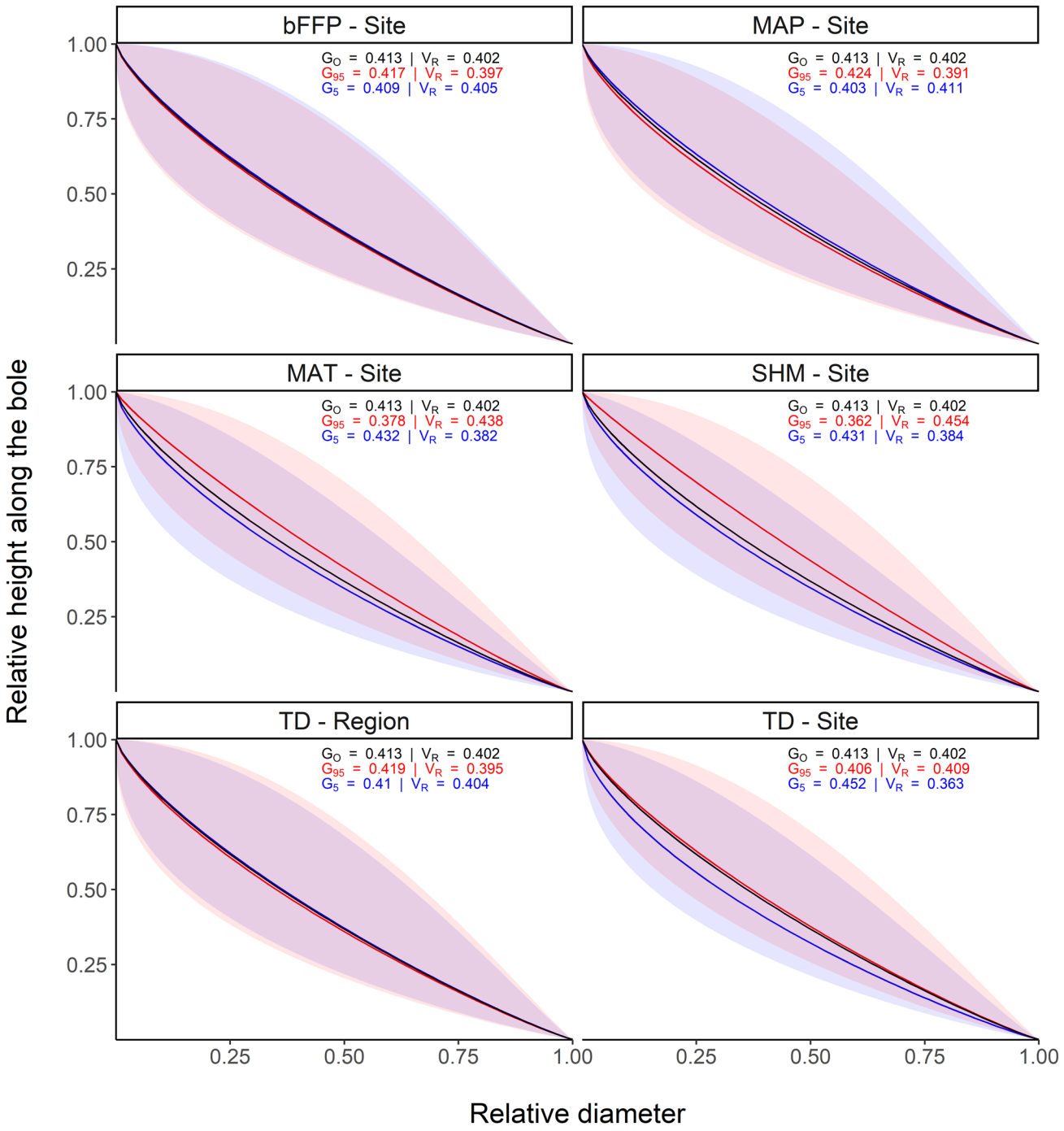

Fig. 3 Modeled tree taper profiles in response to changes in climate variables

in *G* estimates for trees in the final year of the study was 0.204–0.443, a difference in relative volume from 0.65 to 0.41 equivalent to a difference in wood volume of 58%. It is important to note that most predictions of volume growth are based on assumptions of static taper relationships, therefore, the changes in relative volume shown in this study suggest the potential for important impacts on volume production under future climate scenarios in addition to any changes to diameter and height growth that may occur.

Relative changes in *G* estimates from a 2020 baseline for four climate scenarios (RCP4.5 2050 and 2080, RCP8.5 2050 and 2080) are shown in Fig. 4. The climate scenario projections suggest that areas with the highest tapers in 2020 (Sup. Fig. 3) will show increases in taper under all scenarios with more taper at later years and under with the higher

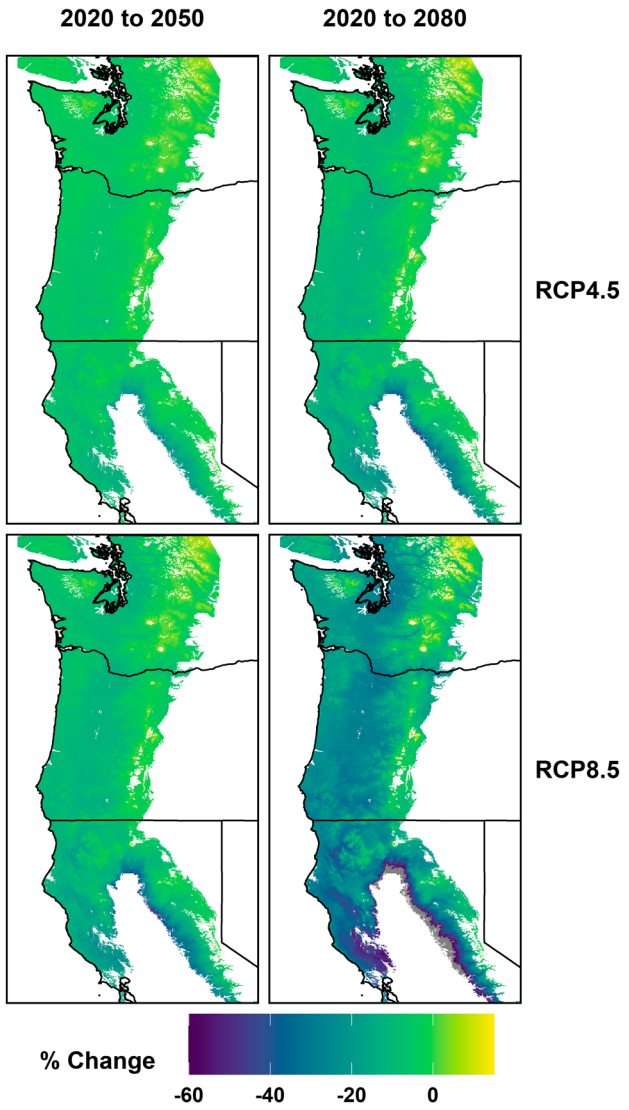

Fig. 4 Percent change in Gini value estimates for indicated timeframes relative to comparable 2020 values under specified emissions scenarios

emissions scenario (RCP8.5). Conversely, the areas with the lowest *G* estimates in 2020 show the largest decreases in *G* estimates in all climate scenarios with greater reductions at later years and the higher emissions scenario. The areas with the highest and lowest *G* estimates are also toward the margins of the range of coast Douglas-fir so the more severe changes shown in Fig. 4 may be indicative of regions that will have future climates near the physiological limits of coast Douglas-fir. This is also suggested by the decline of *G* estimates in Fig. 4, beyond the values shown in Sup. Fig. 3 as indicated by the gray regions in Fig. 4 under the RCP8.5 scenario for year 2080 mostly around the foothills of the California Sierra Nevada. Most of Fig. 4 shows moderate predicted changes in *G*, with more negative changes in later years indicating reductions in taper for most areas in the coast Douglas-fir region under both future climate scenarios.

Discussion

Climate impacts on taper: site

The negative correlation between taper and climate variables SHM, MAP, TD and bFFP below 100 suggest that years with more precipitation, early springs, large differences between warmest and coldest months and hot dry summers lead to reductions in taper. These results could be caused by early budburst associated with cold winter months (high chilling) followed by warm spring temperatures (high forcing) leading to early primary shoot growth without having as much of an impact on secondary growth (i.e., diameter) initiation (Ford et al. 2016). Following a beneficial climate for early shoot growth, and likely growth of the bole within the live crown where carbon is plentiful, hot dry summers may reduce secondary growth or limit its extent (Wensel 2000; Vejpustková and Čihák 2019), thereby increasing the ratio of growth allocated to shoot extension and upper bole growth compared to growth along the lower portion of the bole, thereby reducing tree taper. The switch to a positive correlation between bFFP and taper above a bFFP of 100 is in line with this idea, as higher bFFP values suggest later budburst thereby reducing the shoot extension period and possibly reducing total diameter growth within the crown while not impacting diameter growth lower down. In extreme cases high summer temperature may lead to early diameter cessation (Ford et al. 2017), which could also shift the balance of carbon allocated to shoot extension compared to secondary growth potentially decreasing taper if secondary growth is limited more at the base of the tree than at the top.

The positive correlation between MAT (below 14.7 °C) and taper is similar to what was found in Schneider et al. (2018), and could be related to an extension of the secondary growth period in somewhat warmer years as secondary growth is predicted to initiate earlier under the same future climate scenarios tested in our study (Ford et al. 2016). There is considerable overlap in the Fig. 5(b) of Ford (2016) and Fig. 4 from this study with correlations between areas with increased taper and areas with earlier diameter growth initiation in support of the idea that changes in diameter and height phenology may lead to changes in tree bole taper. The reduction in taper related to SHM is also consistent with the idea that changes in secondary growth phenology are impacting taper, though in looking at summer temperature in combination with photoperiod, secondary growth periods may extend later into the year (Ford et al. 2017). The diameter growth cessation noted by Ford et al. (2017) may also indicate a physiological limit on diameter growth under

high heat periods, possibly explaining the negative relationship between taper and MAT above 14.7 °C where high heat periods would be more likely to occur. The main difference between the findings of Ford (2017) and this study as relates to SHM is that SHM accounts more for moisture availability than does temperature and photoperiod, and reduced water availability can reduce growth (Warren et al. 2005). Given the relative importance of SHM in terms of model sensitivity (Fig. 3) compared to MAT it is likely that moisture availability plays a role in the taper profiles observed.

Bole water in Douglas-fir has been shown to be related to secondary growth with more water available in the upper stem earlier in the year and more water available in the lower bole later in the year (Beedlow et al. 2017). If this distribution of bole water is related to cambial growth along the bole then increasing the growth period late in the year would lead to greater taper and reducing that growth would lead to less taper. This may partially explain the negative relationship with MAP, as increased MAP could increase bole water availability later in the season potentially resulting in less taper depending on where that secondary growth is concentrated. The impacts of climate on taper also appear to vary by species, for instance we found the relationship between MAP and taper for Douglas-fir to be negative while Nigh and Smith (2012) found a positive correlation for *Pinus contorta* Dougl. ex Loud. In addition, Schneider (2018) reported different taper responses to the same climate variables for *Abies balsamea*, *Betula papryifera*, *Picea glauca*, *Picea mariana*, and *Populus tremuloides*, suggesting that taper climate interactions may not be generalizable across species.

Climate impacts on taper: region

The three regional climate variables found in the URFs that make up the best-fit ensemble model were CMD, PAS, and TD. PAS was positively correlated with taper, while TD increased taper above a value of 11.7 °C and reduced taper below that value. This suggests that regions with historically heavy snowfall and high TD values will produce seed-sources that are more tapered compared to seed-sources from regions with little snowfall, and low differences in TD. The interior mountain ranges of the Douglas-fir region typically have higher snowfall than coastal regions in the Douglas-fir range and higher TD, and the interior mountain ranges show generally higher taper values, compared to those found at the coast (Sup. Fig. 2). A greater degree of taper may protect the tree from stem breakage lower in the bole due to the mass of snow that accumulates in the crown. If true that would also partially explain the relationship between PAS and taper, as trees that break lower in the stem would be less likely to reproduce thereby selecting for tree genotypes with more taper.

The negative correlation between CMD, TD (below 11.7), and taper suggest that regions with historically lower ranges in temperature and hot dry conditions are more likely to produce seed-sources with lower taper. This can be seen looking at the trend from lower elevation at the foothills of the interior mountain ranges, where taper is lower, with increasing taper moving up where temperatures tend to be cooler (Sup. Fig. 2). Of the three regional climate variables TD showed the greatest impact on overall taper profiles (Fig. 3), indicating that it may play the largest role in altering taper out of the three regional climate variables. It should be noted that isolating the impacts from individual variables is somewhat difficult given the intertwined nature of the URF models and the ensemble model, in addition to the quadratic form of the URF models and interaction terms within each URF model. That being said, the geographic trends shown in Sup. Fig. 2, a representation of seed-source response, are mostly in agreement with the geographic trends found by St Clair et al. (2005), with lower taper along the coasts, and higher taper inland, as well as generally increasing taper moving south. However, the St. Clair et al. (2005) paper used a different metric for taper (diameter to height ratio) making it difficult to compare results. The mean response by region (Table 2), however, also shows results in general agreement with the St Clair et al. (2005) paper, with hotter dryer regions (e.g., CASIERRA) having lower taper, and colder wetter regions (e.g., WACST) showing higher taper at least for the climates they were exposed to in this study, which did not include any sites in California.

The climate variables within the final ensemble model were not all highly ranked (Table 4) suggesting that more comprehensive variable selection methods are needed to create optimal URF ensemble models rather than relying solely on URF model BIC. The variation in URF predictions demonstrates the importance of using ensemble models to reduce bias (Wang et al. 2010) as the ensemble model can balance different URF responses while still capturing the predictive power of each individual site and seed-source climate URF. This is an important consideration for future trait response studies.

Importance of seed-source population, region and planting site

Planting site explained the most variation of the categorical factors tested, as demonstrated by the large increase in ΔBIC of 1977, and nearly doubling of R^2_c (row 16 vs. row 11 Sup. Table 3). After planting site, region was the next most important explanatory categorical factor increasing ΔBIC by 162 (row 11 vs. 8 Sup. Table 3) with no change in R^2_c. Population level random effects reduced model fit, while random effects for family significantly improved model fit and increased ΔBIC by 18 (row 8 vs. 7 Sup. Table 6) with

no changes in R^2_c. These findings are in line with Krakowski and Stoehr (2009), who found that seed-source regions played a relatively small roll (~ 6%) in explaining trait variation compared to planting site which accounted for 31–60% of the variance, though that study looked at volume and not taper. That study also found significant interaction between genotype and planting site environment, similar to the significant interaction between site and region level climate variables found in this study. The significant interaction effects are an important consideration for overall response of a given seed-source to a planting site climate, in our study four of the five interaction terms had opposite correlations to changes in *G* compared to their respective region climate parameter estimates. This means that the impact of region is moderated by the site-region interaction term, thereby making it harder to detect a region impact in the overall model response. Under these circumstances holding site constant as in Sup Fig. 2, does not result in a consistent relative response from seed-sources as selecting a different site average area would potentially lead to different relative responses between seed-sources.

Range of variability

Taper estimates for populations modeled in their native environments (Sup. Fig. 3) were highly variable although not far outside of the values observed in this study. The lower G values within any given region on Sup. Figure 3 appear to be the hotter drier areas, while higher G values are found in cooler wetter areas. The variation shown in Sup Fig. 3 is driven primarily by the variation in site conditions as the shared map (Sup. Fig. 2) shows less overall variation in *G* values. The map shows that lower elevation, and warmer drier areas have lower taper estimates, while higher elevation and cooler wetter areas have higher taper. This makes sense given the underlying climate variable relationships found in the ensemble model. The range of variation found in Sup. Fig. 3 is also close to the range found in our data with the same lower estimates (0.13) and upper estimates in Sup. Fig. 3 being 13% higher than the upper values observed in this study. This range of variation is higher than that found in St Clair et al. (2005) but given the much larger geographic and climatic conditions in our study, this higher range of variation is not surprising. One important aspect of this range of variation is in the differences in relative volume the range of taper estimates represent. For instance, moving from a *G* estimate of 0.4–0.2 represents a change from a relative volume of ~ 0.4 to ~ 0.65 or approximately a 63% increase in relative volume for a 50% reduction in *G* estimate (Fig. 2). That is a wide range of relative volume values and points to the importance of accounting for taper in bole volume estimation.

The regional variation in G estimates (Sup. Figure 2) was lower than that shown in the site level maps as would be expected given the lower predictive power of region climate variables. However, although this variation was small, it is still important in determining seed-sources that are more likely to produce trees with less taper. In the case of the shared climate map (Sup. Figure 2) those sources are primarily found at the coastal ranges, with some areas of high taper found in the California Klamath range and in the far eastern edge of the coast Douglas-fir range which is likely an area with little coast Douglas-fir present. The trend in taper increasing across a longitudinal gradient from west to east and decreasing along a latitudinal gradient from north to south is similar to what was found in St Clair et al. (2005) and indicates a general adaptation of Douglas-fir to increased taper in hotter drier locations with low snowfall.

Future climate scenarios show a general decline in taper under higher emissions scenarios and later time periods (Fig. 4). That general trend does not tell the whole story though as increases in taper are expected for portions of the Cascade mountain ranges in Oregon and Washington, especially at higher elevations. The greatest decreases in taper occur in California around the perimeter of the Sacramento Valley. Comparing Sup. Fig. 3 with Fig. 4, it appears that areas with low taper in Sup. Fig. 3 are expected to decrease, and areas with high taper are expected to increase in the future. This is most obvious in comparing RCP8.5 2020–2080 in Sup. Fig. 3, where the dark and light areas overlap to a considerable degree. The gray areas in the RPC8.5 2020–2080 (Fig. 4), are likely areas where Douglas-fir will be unable to persist as they result in *G* estimates that are below the minimum observed values in this study. The only way for a tree to achieve extremely low taper is to allocate growth almost entirely to the upper portion of the bole, however, some growth is needed in the lower portion of the bole to maintain enough water conducting sapwood area to maintain foliar water demand, therefore, there is likely a lower limit to taper beyond which trees cannot survive. Projections of future Douglas-fir habitat show very low frequency expected (Gray and Hamann 2013) are in the same areas that are gray in Fig. 4 (RCP8.5 2020–2080 map) suggesting that these low taper projections may be indicative of physiological limits of Douglas-fir. The results from Gray and Hamann (2013) also show reductions in the presence of Douglas-fir in the areas with the highest increase in taper, suggesting that there may be upper and lower taper values that are indicative of physiological limits for the species, and identifying those limits could be useful in projecting the potential for survival of the species under future climates.

Conclusions

Bole taper as estimated using Gini coefficients is significantly influenced by seed-source and planting site climates, with site climates having greater predictive power. The planting site climate variables within the final ensemble model in order of predictive power were: SHM, MAT, TD, MAP, and bFFP. Correlations between these variables and Gini coefficient estimates suggest that cooler years with more precipitation, early springs, large differences between warmest and coldest months and hot dry summers lead to reductions in taper. Model projections under future climate conditions show a general decline in taper in most regions, though regions with the lowest estimated taper in 2020 generally decreased in future time periods and under higher emissions scenarios, and regions with highest taper increased in future time periods and under higher emissions scenarios. The findings from this study have important implications for future relative bole volumes under future climates with varying responses by region.

Author contribution statement BSC and CH planned the experimental design, obtained funding to collect and maintain the D-F Seed-Source Movement Trial, and edited the manuscript. DJ helped collect data, analyzed the data, and wrote the manuscript.

Supplementary Information The online version contains supplementary material available at https://doi.org/10.1007/s00468-021-02254-0.

Funding Funding provided by US Forest Service, and Bureau of Land Management.

Data availability Data available upon request.

Code availability Code available upon request.

References

Bansal S, St. Clair JB, Harrington CA, Gould PJ (2015) Impact of climate change on cold hardiness of Douglas-fir (*Pseudotsuga menziesii*): environmental and genetic considerations. Glob Change Biol 21:3814–3826. https://doi.org/10.1111/gcb.12958

Beedlow PA, Waschmann RS, Lee EH, Tingey DT (2017) Seasonal patterns of bole water content in old growth Douglas-fir (Pseudotsuga menziesii (Mirb.) Franco). Agric for Meteorol 242:109–119. https://doi.org/10.1016/j.agrformet.2017.04.017

Bruchert F, Gardiner B (2006) The effect of wind exposure on the tree aerial architecture and biomechanics of Sitka spruce (Picea sitchensis, Pinaceae). Am J Bot 93:1512–1521. https://doi.org/10.3732/ajb.93.10.1512

Campbell RK, Sugano AI (1993) Genetic variation and seed zones of Douglas-fir in the Siskiyou National Forest. U.S. Department of Agriculture, Forest Service, Pacific Northwest Research Station, Portland

Ceriani L, Verme P (2012) The origins of the Gini index: extracts from Variabilità e Mutabilità (1912) by Corrado Gini. J Econ Inequal 10:421–443. https://doi.org/10.1007/s10888-011-9188-x

Collins M, Knutti R, Arblaster J, et al (2013) Long-term Climate Change: Projections, Commitments and Irreversibility. Clim. Change 2013 Phys. Sci. Basis Contrib. Work. Group Fifth Assess. Rep. Intergov. Panel Clim. Change 1029–1136

del Río M, Bravo-Oviedo A, Ruiz-Peinado R, Condés S (2019) Tree allometry variation in response to intra- and inter-specific competitions. Trees 33:121–138. https://doi.org/10.1007/s00468-018-1763-3

Ford KR, Harrington CA, Bansal S et al (2016) Will changes in phenology track climate change? A study of growth initiation timing in coast Douglas-fir. Glob Change Biol 22:3712–3723. https://doi.org/10.1111/gcb.13328

Ford KR, Harrington CA, St. Clair JB (2017) Photoperiod cues and patterns of genetic variation limit phenological responses to climate change in warm parts of species' range: modeling diameter-growth cessation in coast Douglas-fir. Glob Change Biol 23:3348–3362. https://doi.org/10.1111/gcb.13690

Gray LK, Hamann A (2013) Tracking suitable habitat for tree populations under climate change in western North America. Clim Change 117:289–303. https://doi.org/10.1007/s10584-012-0548-8

Hijmans RJ (2020) raster: geographic data analysis and modeling. Version 3.3–7URL https://CRAN.R-project.org/package=raster. Accessed 10 Jan 2019

King DA (1986) Tree form, height growth, and susceptibility to wind damage in *Acer saccharum*. Ecology 67:980–990

Krakowski J, Stoehr MU (2009) Coastal Douglas-fir provenance variation: patterns and predictions for British Columbia seed transfer. Ann For Sci 66:811–811. https://doi.org/10.1051/forest/2009069

Leites LP, Robinson AP, Rehfeldt GE et al (2012) Height-growth response to climatic changes differs among populations of Douglas-fir: a novel analysis of historic data. Ecol Appl 22:154–165. https://doi.org/10.1890/11-0150.1

McGown KI, O'Hara KL, Youngblood A (2016) Patterns of size variation over time in ponderosa pine stands established at different initial densities. Can J for Res 46:101–113. https://doi.org/10.1139/cjfr-2015-0096

Nigh G, Smith W (2012) Effect of climate on lodgepole pine stem taper in British Columbia, Canada. Forestry 85:579–587. https://doi.org/10.1093/forestry/cps063

Pinheiro J, Bates D, DebRoy S, et al (2019) Linear and nonlinear mixed effects models. Version 3.1–141URL https://CRAN.R-project.org/package=nlme. Accessed 10 Jan 2019

Poorter H, Niklas KJ, Reich PB et al (2012) Biomass allocation to leaves, stems and roots: meta-analyses of interspecific variation and environmental control: Tansley review. New Phytol 193:30–50. https://doi.org/10.1111/j.1469-8137.2011.03952.x

QGIS Development Team (2019) QGIS geographic information system. Version 3.6.3. Open source geospatial foundation. URL: http://qgis.org. Accessed 10 Jan 2019

R Core Team (2019) R: a language and environment for statistical computing. Version 3.5.3. Vienna, Austria. URL https://www.R-project.org/. Accessed 10 Jan 2019

Rehfeldt GE (1994) Evolutionary genetics, the biological species, and the ecology of the Interior cedar–hemlock forests. In: Proceedings of Interior cedar–hemlock–white pine forests: ecology and management. Washington State University, Pullman, WA, pp 91–100

Schneider R, Franceschini T, Fortin M, Saucier J-P (2018) Climate-induced changes in the stem form of 5 North American tree species. For Ecol Manag 427:446–455. https://doi.org/10.1016/j.foreco.2017.12.026

Sorensen FC (1983) Geographic variation in seedling Douglas-Fir (Pseudotsuga Menziesii) from the Western Siskiyou Mountains of Oregon. Ecology 64:696–702. https://doi.org/10.2307/1937191

St Clair JB, Mandel NL, Vance-Borland KW (2005) Genecology of Douglas Fir in Western Oregon and Washington. Ann Bot 96:1199–1214. https://doi.org/10.1093/aob/mci278

Valentine HT, Mäkelä A, Green EJ et al (2012) Models relating stem growth to crown length dynamics: application to loblolly pine and Norway spruce. Trees 26:469–478. https://doi.org/10.1007/s00468-011-0608-0

Vejpustková M, Čihák T (2019) Climate Response of Douglas Fir Reveals Recently Increased Sensitivity to Drought Stress in Central Europe. Forests 10:97. https://doi.org/10.3390/f10020097

Wang T, O'Neill GA, Aitken SN (2010) Integrating environmental and genetic effects to predict responses of tree populations to climate. Ecol Appl 20:153–163. https://doi.org/10.1890/08-2257.1

Wang T, Hamann A, Spittlehouse D, Carroll C (2016) Locally downscaled and spatially customizable climate data for historical and future periods for North America. PLoS One 11:e0156720. https://doi.org/10.1371/journal.pone.0156720

Warren JM, Meinzer FC, Brooks JR, Domec JC (2005) Vertical stratification of soil water storage and release dynamics in Pacific Northwest coniferous forests. Agric for Meteorol 130:39–58. https://doi.org/10.1016/j.agrformet.2005.01.004

Wensel LC (2000) The relationship between tree diameter growth and climate for coniferous species in northern California. Can J for Res 30:1463–1471

White TL, Ching KK (1985) Provenance study of Douglas-fir in the Pacific Northwest region IV. Field performance at age 25 years. Silvae Genet 34:84–90

Yun K, Hsiao J, Jung M-P et al (2017) Can a multi-model ensemble improve phenology predictions for climate change studies? Ecol Model 362:54–64. https://doi.org/10.1016/j.ecolmodel.2017.08.003